

Addressing the LHC flavour anomalies with horizontal gauge symmetries

Andreas Crivellin,¹ Giancarlo D'Ambrosio,^{1,2} and Julian Heeck³

¹*CERN Theory Division, CH-1211 Geneva 23, Switzerland*

²*INFN-Sezione di Napoli, Via Cintia, 80126 Napoli, Italy*

³*Service de Physique Théorique, Université Libre de Bruxelles,
 Boulevard du Triomphe, CP225, 1050 Brussels, Belgium*

We study the impact of an additional $U(1)'$ gauge symmetry with flavour-dependent charges for quarks and leptons on the LHC flavour anomalies observed in $B \rightarrow K^* \mu^+ \mu^-$, $R(K) = B \rightarrow K \mu^+ \mu^- / B \rightarrow K e^+ e^-$, and $h \rightarrow \mu \tau$. In its minimal version with two scalar doublets, the resulting model naturally explains the deviations from the Standard Model observed in $B \rightarrow K^* \mu^+ \mu^-$ and $R(K)$. The CMS access in $h \rightarrow \mu \tau$ can be explained by introducing a third scalar doublet, which gives rise to a prediction for $\tau \rightarrow 3\mu$. We investigate constraints from flavour observables and direct LHC searches for $pp \rightarrow Z' \rightarrow \mu^+ \mu^-$. Our model successfully generates the measured fermion-mixing matrices and does not require vector-like fermions, unlike previous attempts to explain these anomalies.

I. INTRODUCTION

The discovery of a scalar particle at the LHC [1, 2] with properties close to its theoretical prediction within the Standard Model (SM) marks its completion as a description of particle physics. While direct searches for physics beyond the SM were negative at the first LHC run, there are some interesting indirect hints for new physics effects in the flavour sector, namely in the decays of B mesons – $B \rightarrow K^* \mu^+ \mu^-$ and $R(K) = B \rightarrow K \mu^+ \mu^- / B \rightarrow K e^+ e^-$ – and in the decay of the Brout–Englert–Higgs boson $h \rightarrow \mu \tau$.

Specifically, the deviations from the SM found by LHCb [3] in the decay $B \rightarrow K^* \mu^+ \mu^-$ arise mainly in an angular observable called P'_5 [4], with a significance of $2\text{--}3\sigma$ depending on the assumptions for the hadronic uncertainties [5–7]. This effect can be explained in a model-independent effective-field-theory approach by a fairly large contribution of the operator $C_9^{\mu\mu}(\bar{s}\gamma_\alpha P_L b)(\bar{\mu}\gamma^\alpha \mu)$ [8–10].¹ LHCb further observed lepton-non-universality in the B -meson decays [12]

$$R(K) = \frac{B \rightarrow K \mu^+ \mu^-}{B \rightarrow K e^+ e^-} = 0.745_{-0.074}^{+0.090} \pm 0.036, \quad (1)$$

which deviates from the SM prediction $R_K^{\text{SM}} = 1.0003 \pm 0.0001$ [13] by 2.6σ . A possible explanation comes again in the form of a non-zero new-physics contribution to $C_9^{\mu\mu}$ – of the same magnitude as the one required by $B \rightarrow K^* \mu^+ \mu^-$ [6, 14] – as long as the analogous contribution to the corresponding operator with electrons, C_9^{ee} , is small [15–18].

CMS recently presented the results of a search for a lepton-flavour violating (LFV) decay mode of the 125 GeV scalar $h \rightarrow \mu \tau$, with a preferred value [19]

$$\text{Br}[h \rightarrow \mu \tau] = (0.84_{-0.37}^{+0.39}) \%, \quad (2)$$

updating an earlier preliminary result [20]. Since this decay is forbidden in the SM it corresponds to a 2.4σ

deviation. This is particularly exciting because it hints at LFV in the charged-lepton sector, whereas we have so far only observed LFV in the neutrino sector through oscillations. Seeing as the simplest SM extensions that can account for neutrino masses and mixing would not lead to observable $h \rightarrow \mu \tau$ rates, the confirmation of this decay would have a huge impact on our understanding of lepton flavour. In particular, it would imply potentially measurable rates for LFV processes such as $\tau \rightarrow 3\mu$ or $\tau \rightarrow \mu \gamma$ [21–29]. Models aiming to accommodate or explain Eq. (2) rely on an extended scalar sector [30–35] or non-renormalizable effective operators [34, 36, 37].

An explanation for $h \rightarrow \mu \tau$ typically requires additional scalars, while an explanation for $B \rightarrow K^* \mu^+ \mu^-$ requires additional Z' vector bosons (or leptoquarks [16, 38, 39]) to generate the current–current interaction $(\bar{s}\gamma_\alpha P_L b)(\bar{\mu}\gamma^\alpha \mu)$ [40–43]. If the Z' couples non-universally to leptons, it can also account for $R(K) = B \rightarrow K \mu^+ \mu^- / B \rightarrow K e^+ e^-$ [44]. In Ref. [33] we presented a model that can resolve all three anomalies, by combining the model of Ref. [44] (with gauged $U(1)_{L_\mu - L_\tau}$ and effective Z' couplings to quarks generated by heavy vector-quarks) with the one of Ref. [32] (with gauged $U(1)_{L_\mu - L_\tau}$ broken by a second scalar doublet). The combined resolution of the three flavour anomalies gave in particular rise to a prediction for the rate of $\tau \rightarrow 3\mu$.

In this article we want to study the possibility that the same effect employed in Refs. [32, 33] in the lepton sector might also be responsible for flavour violation in the quark sector. Therefore, also the quarks must be charged under the new $U(1)$ gauge group, leading to a model with flavour dependent B and L charges [45–49]. In this way, the introduction of vector-like quarks – which are somewhat “artificially” charged under $L_\mu - L_\tau$ – can be avoided. Furthermore, the model can explain the smallness of the V_{ub} and V_{cb} elements of the Cabibbo–Kobayashi–Maskawa (CKM) mixing matrix. Since the flavour diagonal couplings to quarks are not arbitrary anymore, interesting correlations with LHC searches arise.

The outline of the article is as follows: In the next section, we will consider the possible charge assignments and the symmetry breaking in the quark sector. Sec. III

¹ According to Ref. [11], also underestimated charm effects could explain the deviations from the SM.

is devoted to a phenomenological analysis of the effects in quark flavour physics and direct LHC searches. Sec. IV extends the symmetry breaking to the lepton sector, allowing for a simultaneous explanation of $h \rightarrow \mu\tau$. Finally we conclude in Sec. V. In App. A we briefly discuss related horizontal gauge symmetries.

II. MINIMAL MODEL WITH TWO SCALAR DOUBLETS

Here we study the minimal model with flavour-dependent $U(1)'$ charges which can give rise to the desired effects in $B \rightarrow K^*\mu^+\mu^-$ and $R(K)$. To generate the masses and CKM angles, at least two scalar doublets are necessary.

A. Charge assignment

Concerning leptons, we are drawn to the abelian symmetry $U(1)_{L_\mu-L_\tau}$. It is an anomaly-free global symmetry within the SM [50–52] and also a good zeroth-order approximation for neutrino mixing with a quasi-degenerate mass spectrum, predicting a maximal atmospheric but a vanishing reactor neutrino mixing angle [53–55]. Furthermore, since the Z' boson does not couple to electrons, i.e. $C_9^{ee} = 0$, one naturally obtains an effect of the appropriate size in $R(K)$ once $C_9^{\mu\mu}$ acquires its preferred value from $B \rightarrow K^*\mu\mu$. Therefore, we choose the following assignment for the charges Q' of the new $U(1)'$ gauge group for the lepton generations:

$$Q'(L) = (0, 1, -1). \quad (3)$$

Breaking $L_\mu - L_\tau$ is mandatory for a realistic neutrino sector, and such a breaking can also induce charged LFV processes [56], such as $h \rightarrow \mu\tau$ and $\tau \rightarrow 3\mu$ [32, 33, 57]. However, we postpone the discussion of the symmetry breaking in the charged lepton sector to Sec. IV.

Concerning the quark sector, the first two generations should have the same charges in order to avoid very large effects in $K-\bar{K}$ or $D-\bar{D}$ mixing, generated otherwise unavoidably due to the breaking of the symmetry necessary to generate the Cabibbo angle of the CKM matrix. Furthermore, the first two generations mix much more strongly among themselves than with the third generation, so the latter seems to be somewhat special. If we require in addition the absence of anomalies, we arrive at the following charge assignment for baryons:

$$Q'(B) = (-a, -a, 2a). \quad (4)$$

We will later study the phenomenological implications of different values of a . To reiterate, the $U(1)'$ gauge symmetry we consider is generated by²

$$Q' = (L_\mu - L_\tau) - a(B_1 + B_2 - 2B_3), \quad (5)$$

so the charges are

$$Q' = -\frac{a}{3} \text{ for } u, d, c, s, \quad (6)$$

$$Q' = \frac{2a}{3} \text{ for } t, b, \quad (7)$$

$$Q' = 0 \text{ for } e, \nu_e, \quad (8)$$

$$Q' = 1 \text{ for } \mu, \nu_\mu, \text{ and} \quad (9)$$

$$Q' = -1 \text{ for } \tau, \nu_\tau. \quad (10)$$

Note that the relative coupling strength to quarks and leptons (parametrized by a) is a free parameter because $L_\mu - L_\tau$ and $B_1 + B_2 - 2B_3$ are independently anomaly free. $a \in \mathbb{Q}$ is nevertheless necessary to avoid massless Goldstone bosons (see below). Although not required by anomaly cancellation, we also introduce three right-handed neutrinos ν_R with charges $Q'(\nu_R) = (0, 1, -1)$ to employ a seesaw mechanism for neutrino masses. Other horizontal gauge symmetries can be considered following the above reasoning, but prove less useful in explaining the LHCb anomalies (see App. A).

B. Scalar sector

Two $SU(2)_L$ scalar doublets Ψ_1 and Ψ_2 are introduced to generate viable fermion masses and quark mixing incorporated in the CKM matrix. They carry the $U(1)'$ charges

$$Q'(\Psi_1) = -a \quad \text{and} \quad Q'(\Psi_2) = 0, \quad (11)$$

respectively. Ψ_2 , being uncharged under the $U(1)'$ symmetry, will generate the diagonal entries of the fermion mass matrices as well as the Cabibbo angle. The vacuum expectation value (VEV) $\langle \Psi_1 \rangle$ will generate the mixing between the third and first two quark generations necessary for a viable CKM matrix.

In addition (at least) two SM singlet scalars Φ_1 and Φ_2 with charges

$$Q'(\Phi_1) = 1, \quad Q'(\Phi_2) = -a \quad (12)$$

have to be introduced to break the $U(1)'$ gauge symmetry above the electroweak scale and generate the coupling $\Psi_1^\dagger \Psi_2$ necessary for the mixing of the doublets. The VEV $\langle \Phi_1 \rangle$ will break the $L_\mu - L_\tau$ symmetry in the right-handed neutrino mass matrix relevant for the seesaw mechanism, which leads to a valid neutrino mixing matrix [32, 59]. Φ_2 generates the term $\langle \Phi_2 \rangle \Psi_1^\dagger \Psi_2$ in the scalar potential that leads to the Ψ_1 VEV as well as mixing among Ψ_2 and Ψ_1 .

For a general $a \in \mathbb{R}$, the above particle content leads to a Lagrangian with conserved $U(1)_{L_\mu-L_\tau} \times U(1)_{B_1+B_2-2B_3}$ symmetry. Both the $L_\mu - L_\tau$ symmetries and the $B_1 + B_2 - 2B_3$ are anomaly free and could

² Gauge symmetries that couple to $B_1 + B_2 - 2B_3$ have also been discussed in Ref. [58] with a focus on effects in the up-quark

sector and coupled in the lepton sector not to $L_\mu - L_\tau$, but to the lepton charge $L_e + L_\mu - 2L_\tau$ (which is not a good symmetry in the lepton sector).

be gauged, giving rise to two additional neutral gauge bosons Z' and Z'' which can mix with the SM Z boson [60]. However, we only want to promote the linear combination of Eq. (5) to a gauge symmetry in order to end up with a single Z' that couples to quarks and leptons simultaneously. To remove the orthogonal global $U(1)''$ symmetry, generated by $Q'' = a(L_\mu - L_\tau) + (B_1 + B_2 - 2B_3)$, we have to introduce couplings that connect e.g. Φ_1 and Φ_2 non-trivially. This is only possible for $a \in \mathbb{Q}$ and in general requires the introduction of additional mediator fields. Let us sketch the simplest examples for a , using the fact that the phenomenologically interesting region will be $0 < a < 1$.

- For $a = 1/2$, the potential already allows for a term $\Phi_2^2 \Phi_1$ that breaks the orthogonal global $U(1)''$, so the particle content from above is sufficient to avoid Goldstone modes; a VEV for Φ_2 will induce a VEV for Φ_1 .
- For $a = 1/3$, it is the coupling $\Phi^3 \Phi_1$ that breaks the accidental global $U(1)''$ symmetry explicitly.
- For $a = 1/4$, no dimension-4 operators can be written down with the given scalars that would break the global $U(1)''$. Therefore, one has to introduce a third singlet Φ_3 with $Q'(\Phi_3) = 1/2$, which couples via $\Phi_3^2 \bar{\Phi}_1$ and $\Phi_2^2 \Phi_3$. A Φ_2 VEV will induce a VEV for Φ_3 , which will induce a VEV for Φ_1 .
- For $a = 1/6$, we need Φ_3 with $Q'(\Phi_3) = 1/3$ to couple $\Phi_3^3 \bar{\Phi}_1$ and $\Phi_2^2 \Phi_3$ similar to $a = 1/4$.

The above considerations show that one can easily construct models for various values of $a \in \mathbb{Q}$. However, the details of this procedure will hardly make a difference in our discussion of the phenomenological effects of the doublet scalars and the Z' in the following. Hence, we treat $a \in \mathbb{Q}$ as a free parameter but use $a = 1/2$ and $a = 1/3$ as benchmark values.

Similar to Refs. [32, 33] we consider the limit of small mixing between the heavy singlet scalars Φ_j and the two lighter doublets

$$\Psi_j \equiv \left((v_j + \psi_j^{0,R} \psi_j^\dagger - i\psi_j^{0,I})/\sqrt{2} \right), \quad j = 1, 2. \quad (13)$$

Here, $\psi_{1,2}^{0,R}$ and $\psi_{1,2}^{0,I}$ correspond to the CP-even and the CP-odd components, respectively. For heavy unmixed singlet scalars, we end up with a restricted two-Higgs-doublet model (2HDM) potential of the form

$$\begin{aligned} V \simeq & m_1^2 |\Psi_1|^2 + \frac{\lambda_1}{2} |\Psi_1|^4 + m_2^2 |\Psi_2|^2 + \frac{\lambda_2}{2} |\Psi_2|^4 \\ & + \lambda_{12} |\Psi_1|^2 |\Psi_2|^2 + \tilde{\lambda}_{12} |\Psi_1^\dagger \Psi_2|^2 \\ & + \left(m_{12}^2 \Psi_2^\dagger \Psi_1 + \text{h.c.} \right), \end{aligned} \quad (14)$$

where $m_{12}^2 \propto \mu \langle \Phi_2 \rangle$ is generated by the coupling $\mu \Phi_2 \Psi_1^\dagger \Psi_2$, which induces a small vacuum expectation value for Ψ_1 [32]. We define $v \equiv \sqrt{v_1^2 + v_2^2} \simeq 246$ GeV and $\tan \beta = v_2/v_1$, which is medium to large in the region of interest. The neutral CP-even components $\psi_1^{0,R}$ and

$\psi_2^{0,R}$ mix with an angle α in the usual 2HDM notation to give the mass eigenstates

$$h = \cos \alpha \psi_2^{R,0} - \sin \alpha \psi_1^{R,0}, \quad (15)$$

$$H = \sin \alpha \psi_2^{R,0} + \cos \alpha \psi_1^{R,0}, \quad (16)$$

while the CP-odd components as well as the charged ones mix with β ,

$$A = \cos \beta \psi_2^{0,I} - \sin \beta \psi_1^{0,I}, \quad (17)$$

$$H^- = \cos \beta \psi_2^- - \sin \beta \psi_1^-. \quad (18)$$

Note that in the general 2HDM $-\pi/2 < \alpha < \pi/2$ [61]. We will always assume that h corresponds to the 125 GeV scalar discovered at the LHC [1, 2]. Gauge bosons and leptons have standard type-I 2HDM couplings to the scalars (see for example Ref. [61]).

C. Quark masses and couplings

The $U(1)'$ -neutral scalar doublet Ψ_2 gives flavour diagonal mass terms for quarks and leptons, while Ψ_1 couples only off diagonally to quarks:

$$\mathcal{L}_{Y_q} = -\bar{Q}_f \left(\xi_{fi}^u \tilde{\Psi}_1 + Y_{fi}^u \tilde{\Psi}_2 \right) u_i \quad (19)$$

$$- \bar{Q}_f \left(\xi_{fi}^d \Psi_1 + Y_{fi}^d \Psi_2 \right) d_i + \text{h.c.} \quad (20)$$

Here, Q is the left-handed quark doublet, u is the right-handed up quark and d the right-handed down quark, while i and f label the three generations. We also define the doublets $\tilde{\Psi}_j \equiv i\sigma_2 \Psi_j^*$. The Yukawa couplings Y^u and Y^d of Ψ_2 are forced by our charge assignment to have the form

$$Y^q = \begin{pmatrix} Y_{11}^q & Y_{12}^q & 0 \\ Y_{21}^q & Y_{22}^q & 0 \\ 0 & 0 & Y_{33}^q \end{pmatrix} \quad (21)$$

(with $q = u, d$) and hence allow for the generation of the Cabibbo mixing connecting the first two generations, while the third generation is decoupled. The couplings ξ^q are given by

$$\xi^u = \begin{pmatrix} 0 & 0 & 0 \\ 0 & 0 & 0 \\ \xi_{tu} & \xi_{tc} & 0 \end{pmatrix}, \quad \xi^d = \begin{pmatrix} 0 & 0 & \xi_{db} \\ 0 & 0 & \xi_{sb} \\ 0 & 0 & 0 \end{pmatrix} \quad (22)$$

and lead to the small mixing of the first two generations with the top and bottom quarks after electroweak symmetry breaking. The quark-mass matrices in the interaction eigenbasis are then given by

$$m_u^{\text{EW}} = \frac{v}{\sqrt{2}} (\sin \beta Y^u + \cos \beta \xi^u) \equiv U_L m_u^D U_R^\dagger, \quad (23)$$

$$m_d^{\text{EW}} = \frac{v}{\sqrt{2}} (\sin \beta Y^d + \cos \beta \xi^d) \equiv D_L m_d^D D_R^\dagger, \quad (24)$$

related to the diagonal mass matrices in the physical basis

$$m_u^D = \text{diag}(m_u, m_c, m_t), \quad (25)$$

$$m_d^D = \text{diag}(m_d, m_s, m_b) \quad (26)$$

by the unitary matrices $U_{L,R}$ and $D_{L,R}$. The CKM matrix is then given by the misalignment of the left-handed up and down quark rotations as

$$V \equiv U_L^\dagger D_L. \quad (27)$$

The Lagrangian describing the couplings of quarks to the physical scalar fields is given by

$$\begin{aligned} \mathcal{L} \supset & -\bar{u} \left(\frac{\cos \alpha}{v \sin \beta} m_u^D - \frac{\cos(\alpha - \beta)}{\sqrt{2} \sin \beta} \tilde{\xi}^u \right) P_R u h - \bar{d} \left(\frac{\cos \alpha}{v \sin \beta} m_d^D - \frac{\cos(\alpha - \beta)}{\sqrt{2} \sin \beta} \tilde{\xi}^d \right) P_R d h \\ & -\bar{u} \left(\frac{\sin \alpha}{v \sin \beta} m_u^D - \frac{\sin(\alpha - \beta)}{\sqrt{2} \sin \beta} \tilde{\xi}^u \right) P_R u H - \bar{d} \left(\frac{\sin \alpha}{v \sin \beta} m_d^D - \frac{\sin(\alpha - \beta)}{\sqrt{2} \sin \beta} \tilde{\xi}^d \right) P_R d H \\ & -i\bar{u} \left(\frac{m_u^D}{v \tan \beta} - \frac{1}{\sqrt{2} \sin \beta} \tilde{\xi}^u \right) P_R u A + i\bar{d} \left(\frac{m_d^D}{v \tan \beta} - \frac{1}{\sqrt{2} \sin \beta} \tilde{\xi}^d \right) P_R d A \\ & -\bar{u} \left[\left(\frac{\sqrt{2}}{v \tan \beta} m_u^D V - \frac{1}{\sin \beta} (\tilde{\xi}^u)^\dagger V \right) P_L + \left(\frac{\sqrt{2}}{v \tan \beta} V m_d^D - \frac{1}{\sin \beta} V \tilde{\xi}^d \right) P_R \right] d H^+, \end{aligned} \quad (28)$$

where we omitted the hermitian conjugated terms and flavour indices. In addition we defined the non-diagonal coupling matrices

$$\tilde{\xi}^u = U_L^\dagger \xi^u U_R, \quad \tilde{\xi}^d = D_L^\dagger \xi^d D_R. \quad (29)$$

The terms proportional to m_q^D correspond to the usual type-I 2HDM-like couplings, while the terms involving ξ^q induce flavour violation and will be regarded as small perturbations with respect to the type-I structure.

Since ξ_{31}^u and ξ_{32}^u correspond to right-handed rotations, the CKM matrix is (to a good approximation) given by $V \simeq D_L$, while the mixing angles in D_R generated by ξ_{13}^d and ξ_{23}^d are suppressed to those in D_L by $m_{d,s}/m_b$, and so $D_R \simeq \mathbb{I}$. A perturbative diagonalization of the quark mass matrices gives

$$\xi_{db} \simeq \frac{\sqrt{2}}{\cos \beta} \frac{m_b}{v} V_{ub}, \quad \xi_{sb} \simeq \frac{\sqrt{2}}{\cos \beta} \frac{m_b}{v} V_{cb}, \quad (30)$$

in particular $\xi_{db}/\xi_{sb} \ll 1$. For medium to large values of $\tan \beta$, our model explains why V_{ub} and V_{cb} are much smaller than the Cabibbo angle as the contributions of ξ_{sb} and ξ_{db} to the mass matrix are suppressed by $\tan \beta$.³ The non-diagonal matrix relevant for all the scalar couplings is then given by

$$\tilde{\xi}^d \simeq V^\dagger \xi^d \simeq \frac{\sqrt{2}}{\cos \beta} \frac{m_b}{v} \begin{pmatrix} 0 & 0 & -V_{td}^* V_{tb} \\ 0 & 0 & -V_{ts}^* V_{tb} \\ 0 & 0 & 1 - |V_{tb}|^2 \end{pmatrix}. \quad (31)$$

The dominant flavour off-diagonal coupling is that to sb , while that to db is suppressed by $V_{td}/V_{ts} \simeq 0.2$. Note

that the flavour-violating couplings are entirely given in terms of the CKM matrix elements. Therefore, flavour violation in the down-quark sector induced by the scalars only involves the free parameters $\tan \beta$, α and the scalar masses, making our model highly predictive.

While the couplings ξ_{23}^d and ξ_{13}^d are fixed by the requirement that the measured CKM matrix is generated, the couplings ξ_{31}^u and ξ_{32}^u are free parameters generating top-quark flavor-changing effects not under investigation in this analysis. We therefore neglect their effect in the following and set $\xi^u = 0$. One should keep in mind that these couplings can in principle induce decays such as $t \rightarrow hc$ and $t \rightarrow hu$. However, as we will see, the scalar-mixing angle α must be very small in order not to violate bounds from $B_s - \bar{B}_s$ mixing, rendering the h - q - q couplings nearly SM-like. Therefore, also the effect in $t \rightarrow hc$ and $t \rightarrow hu$ is suppressed.

The Z' couplings to up quarks are vector-like in the limit $\xi^u = 0$ we consider in this paper

$$g' \bar{u} \gamma^\mu \text{diag}(-a/3, -a/3, 2a/3) u Z'_\mu. \quad (32)$$

Due to the rotation $D_L \simeq V$, the Z' couplings to down quarks are chiral and given by

$$g' (\bar{d}_i \gamma^\mu P_L d_j Z'_\mu \Gamma_{ij}^{dL} + \bar{d}_i \gamma^\mu P_R d_j Z'_\mu \Gamma_{ij}^{dR}), \quad (33)$$

with coupling matrices

$$\Gamma^{dL} \simeq a \begin{pmatrix} |V_{td}|^2 - \frac{1}{3} & V_{ts} V_{td}^* & V_{tb} V_{td}^* \\ V_{td} V_{ts}^* & |V_{ts}|^2 - \frac{1}{3} & V_{tb} V_{ts}^* \\ V_{td} V_{tb}^* & V_{ts} V_{tb}^* & |V_{tb}|^2 - \frac{1}{3} \end{pmatrix}, \quad (34)$$

$$\Gamma^{dR} \simeq a \begin{pmatrix} -1/3 & 0 & 0 \\ 0 & -1/3 & 0 \\ 0 & 0 & 2/3 \end{pmatrix}. \quad (35)$$

³ Demanding perturbatively small values for $\xi_{db, sb}$ yields a mild upper bound $\tan \beta < \mathcal{O}(10^3)$ due to the smallness of $V_{ub, cb}$.

Note that this reduces to $\text{diag}(-a/3, -a/3, 2a/3)$ also for the left-handed couplings in the limit in which the CKM

matrix is the unit matrix. As the right-handed couplings are to a good approximation flavour diagonal, this will ultimately lead to the desired hierarchy $|C'_9| \ll |C_9|$ hinted at by global fits [6, 8, 62]. Note that an opposite $U(1)'$ charge for Ψ_1 would require the CKM matrix to be generated in the up sector, while right-handed down-quark Z' couplings would be free parameters, rendering the left-handed down-quark Z' couplings flavour conserving. As we will see in the next section, one cannot explain $R(K)$ and $B \rightarrow K^* \mu\mu$ in such a setup. Also note that the coupling matrix Γ^{dL} is hermitian with complex off-diagonal entries. This will in principle lead to quark-dipole moments [63], which are, however, proportional to $\Gamma_{ij}^L \Gamma_{ij}^{R*}$ (with $i \neq j$) and hence vanishingly small in our scenario with diagonal Γ^R .

It is important to reiterate that our model has, by construction, suppressed flavour violation between the first two generations, which drastically softens constraints. Furthermore, the “detached” third quark generation is motivated by the observed smaller mixing angles.

D. Lepton masses and couplings

Since we only consider $|a| < 1$ in order to avoid stringent constraints from $\Delta F = 2$ processes, it is not possible to couple the scalar doublet Ψ_1 with $U(1)'$ charge a to leptons. The Dirac mass matrices for the leptons are hence generated by Ψ_2 only and are diagonal in flavour space due to the charge assignment of our $U(1)'$ symmetry. There is hence no charged-lepton flavor violation in this simple 2HDM. However, extending the model by a third doublet with $|Q'| = 2$ (Sec. IV) can again lead to LFV and in particular give rise to the decay $h \rightarrow \mu\tau$, as pointed out in Refs. [32, 33]. For now, we consider the 2HDM with charged-lepton flavour conservation.

Neutrino masses arise via the seesaw mechanism [68] as $m_\nu \simeq -m_D m_R^{-1} m_D^T$ with diagonal Dirac mass matrix $m_D \propto \langle \Psi_2 \rangle$ and the right-handed Majorana neutrino mass matrix given by [59]

$$m_R = \begin{pmatrix} M_1 & a_{12} \langle \Phi_1 \rangle & a_{13} \langle \Phi_1 \rangle \\ a_{12} \langle \Phi_1 \rangle & 0 & M_2 \\ a_{13} \langle \Phi_1 \rangle & M_2 & 0 \end{pmatrix}. \quad (36)$$

As a consequence of our minimal singlet sector, two texture zeros in m_R remain and propagate to m_ν as two vanishing minors [59]: $(m_\nu^{-1})_{22} = 0 = (m_\nu^{-1})_{33}$. These zeros lead to relations among the neutrino mixing parameters that allow us to predict the unknown phases and masses given the measured neutrino mixing angles and the mass-squared differences [69, 70]. In our case we predict normal ordering, typically with quasi-degenerate masses. Delicate cancellations can, however, occur which lead to a normal hierarchy (see Fig. 1). With the best-fit values for Δm_{ij}^2 and θ_{ij} from the global fit of Ref. [64], we predict the lightest neutrino mass to be $m_1 = 0.076$ eV, and hence $\sum_j m_j = 0.24$ eV, as well as $|\sin \delta_{\text{CP}}| = 0.96$, and $m_{\beta\beta} \equiv |(m_\nu)_{ee}| = 0.065$ eV. Note that this prediction for δ_{CP} agrees well with the preferred region from the global fit, $\delta_{\text{CP}}/^\circ = 306_{-70}^{+39}$ [64]. Using the 3σ ranges

for mixing angles and Δm_{ij}^2 , we obtain lower bounds on the neutrino mass observables

$$\sum_j m_j \gtrsim 0.095 \text{ eV}, \quad m_{\beta\beta} \gtrsim 9.5 \text{ meV}. \quad (37)$$

The sum of neutrino masses $\sum_j m_j$ is large enough to have a cosmological impact [71]; in fact, Planck already constrains $\sum m < 0.23$ eV at 95% C.L. [66, 67], which, however, depends strongly on the combination of data sets. The effective neutrino mass $m_{\beta\beta}$ relevant for neutrinoless double-beta decay is also in the reach of future experiments (see Ref. [72] for a recent review). There is a strong correlation between the CP phase and the atmospheric mixing angle, approximately given by

$$\delta_{\text{CP}} \simeq \begin{cases} 90^\circ + 360^\circ (\sin^2 \theta_{23} - 1/2), \text{ or} \\ 270^\circ - 360^\circ (\sin^2 \theta_{23} - 1/2). \end{cases} \quad (38)$$

For a more extensive discussion of this neutrino structure, we refer to Refs. [69, 70]. Despite the lack of charged lepton flavour violation, our simple 2HDM is hence testable in the lepton sector as well.

Let us come to the scalar–lepton interactions. Since Ψ_1 has no couplings to leptons, the couplings of h , H , A , and H^+ are given simply by those of a type-I 2HDM, i.e.

$$\begin{aligned} \mathcal{L} \supset & -\bar{e} \left(\frac{\cos \alpha}{v \sin \beta} m_e^D \right) e h - \bar{e} \left(\frac{\sin \alpha}{v \sin \beta} m_e^D \right) e H \\ & - i\bar{e} \left(\frac{m_e^D}{v \tan \beta} \right) \gamma_5 e A \\ & - \left[\bar{\nu} \left(\frac{\sqrt{2}}{v \tan \beta} U^\dagger m_e^D \right) P_R e H^+ + \text{h.c.} \right], \end{aligned} \quad (39)$$

with the Pontecorvo–Maki–Nakagawa–Sakata mixing matrix U and $m_e^D \equiv \text{diag}(m_e, m_\mu, m_\tau)$. Here, we ignored the couplings to the right-handed neutrinos, assuming them to be very heavy. For the charged-lepton couplings to Z' , we have the usual vectorial $L_\mu - L_\tau$ couplings

$$g' (\bar{e}_i \gamma^\mu P_L e_j Z'_\mu \Gamma_{ij}^{eL} + \bar{e}_i \gamma^\mu P_R e_j Z'_\mu \Gamma_{ij}^{eR}), \quad (40)$$

with

$$\Gamma_{fi}^{eL} = \Gamma_{fi}^{eR} = \begin{pmatrix} 0 & 0 & 0 \\ 0 & 1 & 0 \\ 0 & 0 & -1 \end{pmatrix}, \quad (41)$$

which are flavour-conserving in this minimal 2HDM (lepton-flavour violation will arise in the 3HDM of Sec. IV).

E. Gauge boson sector

The Z' mass in case of just two singlet scalars (see Eq. (12)) is given in the limit of interest $\langle \Phi_j \rangle \gg \langle \Psi_i \rangle$ by

$$m_{Z'}^2 \simeq 2g'^2 (\langle \Phi_1 \rangle^2 + a^2 \langle \Phi_2 \rangle^2). \quad (42)$$

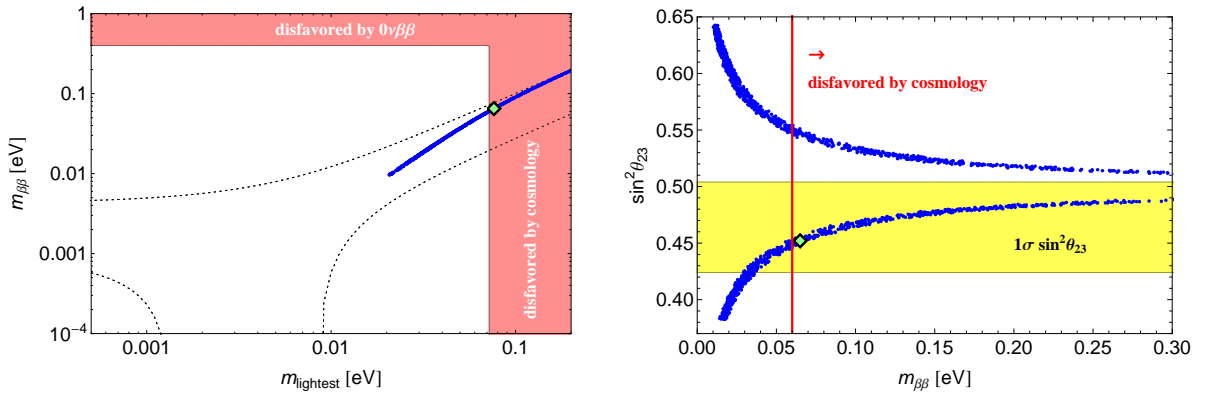


FIG. 1: Left: $m_{\beta\beta}$ vs. lightest neutrino mass (in blue) as predicted by the two vanishing minors $(m_\nu^{-1})_{22} = 0 = (m_\nu^{-1})_{33}$ in combination with the 3σ values for θ_{ij} and Δm_{ij}^2 from Ref. [64]. The diamond marks the best-fit point. The dotted black lines show the standard allowed 3σ range for normal ordering. The red regions are disfavored by GERDA [65] (conservative limit) and Planck [66, 67]. Right: Correlation of $\sin^2\theta_{23}$ with $m_{\beta\beta}$ due to the two vanishing minors. The yellow region denotes the 1σ range for θ_{23} , and the diamond marks the best-fit point.

Ignoring kinetic mixing between $U(1)'$ and hypercharge $U(1)_Y$, a Z - Z' mixing angle $\theta_{ZZ'}$ [73] is nevertheless induced by the VEV of Ψ_1 [32],

$$g'\theta_{ZZ'} \simeq -\frac{ag_1 v^2 \cos^2 \beta}{2m_{Z'}^2/g'^2} \simeq -2 \times 10^{-4} a \left(\frac{10}{\tan \beta}\right)^2 \left(\frac{\text{TeV}}{m_{Z'}/g'}\right)^2. \quad (43)$$

The gauge eigenstates Z and Z' can then be expressed in terms of the mass eigenstates Z_1 and Z_2 as

$$Z \simeq Z_1 - \theta_{ZZ'} Z_2, \quad (44)$$

$$Z' \simeq Z_2 + \theta_{ZZ'} Z_1, \quad (45)$$

which couple to

$$-\mathcal{L} \supset (g_1 j_{1,\mu} + g'\theta_{ZZ'} j'_\mu) Z_1^\mu + (g' j'_\mu - g_1 \theta_{ZZ'} j_{1,\mu}) Z_2^\mu, \quad (46)$$

where $g_1 \equiv g/c_W = e/s_W c_W$ (with $s_W = \sin \theta_W$ etc. for the weak mixing angle θ_W) and the SM neutral current [73]

$$j_1^\mu = \sum_f \bar{f} \gamma^\mu [(t_3(f) - s_W^2 Q(f)) P_L - s_W^2 Q(f) P_R] f. \quad (47)$$

The $U(1)'$ current j'_μ is given in Eqs. (32), (33), and (40).

In the lepton sector, this Z - Z' mixing leads to small vector-coupling shifts of the light Z_1 (i.e. the SM Z studied at LEP) to muons and taus,

$$g_V^Z(\mu\mu, \tau\tau) \simeq -1/2 + 2s_W^2 \pm g'\theta_{ZZ'}/g_1, \quad (48)$$

and thus ultimately to lepton-flavour non-universality in the Z couplings [56]. Simply demanding that the additional contribution does not exceed three times the 1σ error ($g_V^Z(\tau\tau) = -0.0366 \pm 0.0010$) gives

$$|g'\theta_{ZZ'}| \lesssim g_1 0.003 \simeq 2 \times 10^{-3}, \quad (49)$$

easily satisfied for the parameters under investigation (see Eq. (43)).

The Z also inherits the Z' quark couplings and thus contributes to flavor violation in the quark sector. Its contribution will be enhanced by its smaller mass but suppressed by $\theta_{ZZ'}$. For TeV scale Z' , the mass-enhancement cannot overcome the Z - Z' mixing suppression, so we ignore the flavour-changing Z couplings in the following.

Since the Z - Z' mixing angle is small, we will continue to denote the new gauge boson by Z' in the following. As we assume the three right-handed neutrinos to be heavier than the Z' , the invisible branching ratio is set by the active neutrinos,

$$\text{Br}[Z' \rightarrow \text{inv}] = \frac{\sum_\nu \Gamma[Z' \rightarrow \nu\nu]}{\sum_f \Gamma[Z' \rightarrow ff]} \simeq \frac{1}{3 + 4a^2}, \quad (50)$$

assuming $m_t \ll m_{Z'} < 2m_{\nu_R}$. In the same limit, we have

$$\text{Br}[Z' \rightarrow \mu\mu] \simeq \text{Br}[Z' \rightarrow \tau\tau] \simeq \frac{1}{3 + 4a^2}, \quad (51)$$

while the branching ratio into two up quarks (same for d , s , c) is $a^2/3$ times the above, that into top quarks (same for bottom) is $4a^2/3$ times the above.

III. FLAVOUR OBSERVABLES AND LHC CONSTRAINTS

We will now investigate the relevant bounds on our model, i.e. B -meson decays, $\Delta F = 2$ processes, neutrino trident production, and direct LHC searches. We will not go into details about the standard phenomenology of 2HDMs of type I (see Refs. [74, 75] for a recent evaluation) but rather discuss constraints arising from the deviations from the type-I structure due to the additional flavour violation.

A. $B \rightarrow K^* \mu^+ \mu^-$ and $B \rightarrow K \mu^+ \mu^- / B \rightarrow K e^+ e^-$

Concerning leptonic B decays, both $B \rightarrow K^* \mu^+ \mu^-$ and $R(K)$ are sensitive to the Wilson coefficients $C_9^{(\prime)\mu\mu}$ and $C_{10}^{(\prime)\mu\mu}$ incorporated in the effective Hamiltonian,

$$\mathcal{H}_{\text{eff}} = -\frac{4G_F}{\sqrt{2}} V_{tb} V_{ts}^* \left(\sum_{j=9,10} C_j^{\ell\ell} O_j^{\ell\ell} + C_j^{\prime\ell\ell} O_j^{\prime\ell\ell} \right) + \text{h.c.}, \quad (52)$$

with

$$\begin{aligned} O_9^{\ell\ell} &= \frac{\alpha_{\text{EM}}}{4\pi} [\bar{s}\gamma^\mu P_L b] [\bar{\ell}\gamma_\mu \ell], \\ O_9^{\prime\ell\ell} &= \frac{\alpha_{\text{EM}}}{4\pi} [\bar{s}\gamma^\mu P_R b] [\bar{\ell}\gamma_\mu \ell], \\ O_{10}^{\ell\ell} &= \frac{\alpha_{\text{EM}}}{4\pi} [\bar{s}\gamma^\mu P_L b] [\bar{\ell}\gamma_\mu \gamma^5 \ell], \\ O_{10}^{\prime\ell\ell} &= \frac{\alpha_{\text{EM}}}{4\pi} [\bar{s}\gamma^\mu P_R b] [\bar{\ell}\gamma_\mu \gamma^5 \ell], \end{aligned} \quad (53)$$

with $\ell \in \{e, \mu, \tau\}$. In our model we generate the two coefficients $C_9^{\mu\mu} = -C_9^{\tau\tau}$ with

$$C_9^{\mu\mu} \simeq \frac{-g'^2}{\sqrt{2}m_{Z'}^2} \frac{\pi}{\alpha_{\text{EM}}} \frac{1}{G_F} a \simeq -\left(\frac{a}{1/3}\right) \left(\frac{3 \text{ TeV}}{m_{Z'}/g'}\right)^2, \quad (54)$$

while

$$C_9^{ee} = C_9^{\prime\ell\ell} = C_{10}^{\ell\ell} = C_{10}^{\prime\ell\ell} = 0. \quad (55)$$

Note that $C_9^{\mu\mu}$ is real in our model but could have either sign depending on a . As already noted in Refs. [8, 62], $C_9^{\mu\mu} < 0$ and $C_9^{\mu\mu} = 0$ gives a good fit to data. Using the global fit of Ref. [6] we see that at (1σ) 2σ level

$$-0.60 (-0.95) \geq C_9^{\mu\mu} \geq (-1.65) - 2.00, \quad (56)$$

with a best-fit value $C_9^{\mu\mu} \simeq -1.3$. Interestingly, the regions for $C_9^{\mu\mu}$ required by $R(K)$ and $B \rightarrow K^* \mu^+ \mu^-$ lie approximately in the same region. A Z' explanation of $R(K)$ and $B \rightarrow K^* \mu^+ \mu^-$ has also been considered in Ref. [6] as an effective model, with similar constraints as presented here.

Putting everything together, we find the 2σ preferred region for our model from $R(K)$ and $B \rightarrow K^* \mu^+ \mu^-$

$$2.3 \frac{m_{Z'}^2}{(10 \text{ TeV})^2} \leq ag'^2 \leq 7.7 \frac{m_{Z'}^2}{(10 \text{ TeV})^2}, \quad (57)$$

with best-fit value $m_{Z'}/\sqrt{ag'} = 4.5 \text{ TeV}$. In the following we discuss additional constraints on a , g' and $m_{Z'}$ that are of relevance to our resolution of the LHCb anomalies.

B. $\Delta F = 2$ processes

The Z' and scalars have flavour non-diagonal couplings, generating tree-level contributions to $\Delta F = 2$ processes. Considering for definiteness $B_s - \bar{B}_s$ mixing ($B_d - \bar{B}_d$ and $K - \bar{K}$ follow by simple replacements of indices),

the relevant effective Hamiltonian is conventionally written as (see for example Refs. [76, 77])

$$\mathcal{H}_{\text{eff}}^{\Delta F=2} = \sum_{j=1}^5 C_j O_j + \sum_{j=1}^3 C_j' O_j' + \text{h.c.}, \quad (58)$$

with

$$\begin{aligned} O_1 &= [\bar{s}_\alpha \gamma^\mu P_L b_\alpha] [\bar{s}_\beta \gamma^\mu P_L b_\beta], \\ O_2 &= [\bar{s}_\alpha P_L b_\alpha] [\bar{s}_\beta P_L b_\beta], \\ O_3 &= [\bar{s}_\alpha P_L b_\beta] [\bar{s}_\beta P_L b_\alpha], \\ O_4 &= [\bar{s}_\alpha P_L b_\alpha] [\bar{s}_\beta P_R b_\beta], \\ O_5 &= [\bar{s}_\alpha P_L b_\beta] [\bar{s}_\beta P_R b_\alpha]. \end{aligned} \quad (59)$$

Here, α and β are color indices, and the primed operators are obtained by the exchange $L \leftrightarrow R$.

In our model we find the contributions (using the expression for C_2' given in Ref. [77])

$$C_1 = \frac{g'^2}{2m_{Z'}^2} (\Gamma_{sb}^{dL})^2, \quad C_2' = \sum_{\eta=h,H,A} \frac{-1}{2m_\eta^2} (\Gamma_{sb}^\eta)^2, \quad (60)$$

while all other Wilson coefficients are zero. It is important to note that the Z' contribution to the $\Delta F = 2$ processes scales like $a^2 g'^2 / m_{Z'}^2$, while the contribution to leptonic decays, such as $B \rightarrow K \mu \mu$, are proportional to $ag'^2 / m_{Z'}^2$. This makes it possible to evade $\Delta F = 2$ constraints by choosing $a \ll 1$, while still accommodating the LHCb anomalies. As we will see below, $a \lesssim 1$ is actually already sufficient for this purpose.

The Wilson coefficients C_j enter physical observables, i.e. mass differences and CP asymmetries, via the calculation of matrix elements involving decay constants and bag factors calculated with lattice QCD (see for example Ref. [78] for a review of recent lattice values). In addition, the QCD renormalization group effects must be taken into account. For this we use the next-to-leading-order equations calculated in Refs. [76, 79].

On the experimental side, the central values of Δm_{B_s} and Δm_{B_d} are slightly above the SM prediction, and the same is true for ε_K extracted from $K - \bar{K}$ mixing. This is interesting since our model predicts necessarily constructive interference of the Z' contribution with the SM in all three observables. For our numerical values, we use the 95% C.L. results of the UTfit collaboration [80–82]:

$$0.76 < R_{B_d} = \Delta m_{B_d} / \Delta m_{B_d}^{\text{SM}} < 1.43, \quad (61)$$

$$0.90 < R_{B_s} = \Delta m_{B_s} / \Delta m_{B_s}^{\text{SM}} < 1.23, \quad (62)$$

$$0.77 < R_{\varepsilon_K} = \varepsilon_K / \varepsilon_K^{\text{SM}} < 1.41. \quad (63)$$

Similar results are obtained by the CKMfitter collaboration [83].

The strongest constraints come from B_s mixing, as can be seen in Fig. 2, but can easily be evaded for $a < 1$ even for the large $|C_9^{\mu\mu}| \sim 1$ required to explain the B -meson anomalies. Similar but weaker bounds hold for the other $\Delta F = 2$ processes. From $B_s - \bar{B}_s$ mixing we get the approximate 95% C.L. bound

$$a^2 g'^2 \leq 2.6 \frac{m_{Z'}^2}{(10 \text{ TeV})^2}. \quad (64)$$

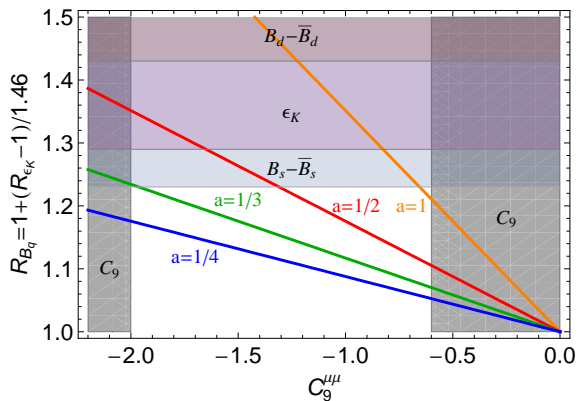


FIG. 2: R_{B_q} and R_{ϵ_K} as a function of $C_9^{\mu\mu}$ for different values of a taking into account the Z' contribution only. The horizontal gray regions are excluded by Δm_{B_q} and ϵ_K , while the vertical ones are excluded by $B \rightarrow K^* \mu^+ \mu^-$ and $R(K)$. We used $m_{Z'} = 3$ TeV for the renormalization group for the $\Delta F = 2$ processes. Note that the dependence on $m_{Z'}$ is therefore only logarithmic.

Note that this bound is obtained for $m_{Z'} = 10$ TeV and only scales approximately like $m_{Z'}^2$, due to the additional logarithmic dependence on the mass from the renormalization group.

The flavour-changing neutral scalar couplings also affect Δm_{B_s} (and also Δm_{B_q} and Δm_K). Here, the H, A contributions decouple as $1/m_{H,A}^2$, while the h contribution vanishes for $\alpha - \beta = \pi/2$. For large values of $\tan \beta$ and small α we have approximately

$$\frac{\Delta m_{B_s}^{h,H,A}}{\Delta m_{B_s}^{\text{SM}}} \simeq 0.12 \cos^2(\alpha - \beta) \tan^2 \beta + 0.19 \tan^2 \beta \left(\frac{(200 \text{ GeV})^2}{m_H^2} - \frac{(200 \text{ GeV})^2}{m_A^2} \right). \quad (65)$$

The allowed regions in the $\tan \beta - \alpha$ plane are shown in the right plot of Fig. 3 assuming that the Z' generates the central value of $C_9^{\mu\mu}$ for $a = 1/3$. One can see that the bounds are weaker if $m_A < m_H$ and stronger for $m_A > m_H$ due to the negative A contribution in Eq. (65).

C. Neutrino trident production

The most stringent bound on flavour-diagonal Z' couplings to muons only (i.e. no quark or electron couplings) arises from neutrino trident production (NTP) $\nu_\mu N \rightarrow \nu_\mu N \mu^+ \mu^-$ [44, 85]:

$$\frac{\sigma_{\text{NTP}}}{\sigma_{\text{NTP}}^{\text{SM}}} \simeq \frac{1 + \left(1 + 4s_W^2 + 8 \frac{g'^2}{m_{Z'}^2} \frac{m_W^2}{g_2^2}\right)^2}{1 + (1 + 4s_W^2)^2}. \quad (66)$$

Taking only the CCFR data [86], we find roughly $m_{Z'}/g' \gtrsim 550$ GeV at 95% C.L. for a heavy Z' . This cuts slightly into the parameter space allowed by B_s mixing and C_9 but is only relevant for $a \ll 1$ (see Fig. 5).

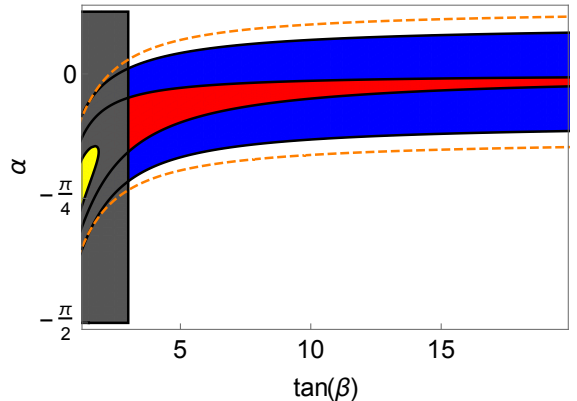


FIG. 3: Allowed regions in the $\tan \beta - \alpha$ plane assuming that $C_9^{\mu\mu}$ is reproduced by the Z' contribution within 2σ for $a = 1/3$ for $m_H = 300$ GeV and $m_A = 350$ GeV (yellow), $m_A = 300$ GeV (red) and $m_A = 250$ GeV (blue). The gray region is excluded by $b \rightarrow s\gamma$ [84]. Dashed lines indicate $\cos(\alpha - \beta) = \pm 0.4$ for reference.

D. Direct LHC searches

Since (unlike in Refs. [33, 44]) we have (potentially sizable) Z' couplings to the first-generation quarks, our model is constrained by LHC searches for $pp \rightarrow Z' \rightarrow \mu\mu$. With vectorial Z' couplings, universal in the first four quark generations, our model is closely related to $U(1)_{B-L}$ models [87], for which dedicated analyses exist. Working in the narrow-width approximation, the relevant quantity for collider searches is the Drell-Yan production cross section times branching ratio into muons,

$$\frac{\sigma(pp \rightarrow Z') \text{BR}[Z' \rightarrow \mu\mu]}{\sigma(pp \rightarrow Z'_{B-L}) \text{BR}[Z'_{B-L} \rightarrow \mu\mu]} \simeq \frac{a^2 g'^2}{g_{B-L}^2} \frac{1/(3+4a^2)}{2/13}, \quad (67)$$

valid for $m_t \ll m_{Z'} < 2m_{\nu_R}$. One can therefore simply rescale the $B-L$ limits of ATLAS's $\sqrt{s} = 8$ TeV analysis of di-muon resonance searches (see auxiliary figures of Ref. [88]), resulting in Fig. 4. Contrary to low-energy observables – which only depend on the ratio $g'^2/m_{Z'}^2$ – the LHC probes on-shell Z' . This leads to a complicated dependence on $m_{Z'}$, since the production cross section involves parton-density functions. As a result, the production cross section, and therefore the sensitivity, decreases strongly once $m_{Z'}$ approaches the maximal available energy.

For $a \ll 1$ (i.e. the leptophilic case), the Drell-Yan production becomes negligible, and our model again resembles the standard $L_\mu - L_\tau$ models. In this case, the Z' production at colliders goes through $pp \rightarrow \mu\mu Z' \rightarrow 4\mu$ (or 3μ plus missing energy), where the Z' is radiated off a final state lepton [89]. For $m_{Z'} > m_Z$, the LHC constraints are currently weaker than NTP [44] but will become competitive with higher luminosities [90–92].

Finally, for Z' masses above the on-shell threshold, one can obtain limits from searches for contact interactions,

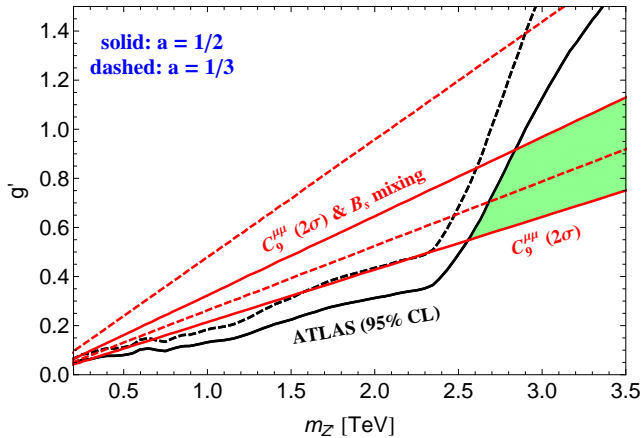


FIG. 4: Limits on $q\bar{q} \rightarrow Z' \rightarrow \mu\bar{\mu}$ from ATLAS [88] (black, allowed region down right) and the 2σ limits on $C_9^{\mu\mu}$ to accommodate $B \rightarrow K^*\mu^+\mu^-$ and $B \rightarrow K\mu^+\mu^-/B \rightarrow Ke^+e^-$ (red, allowed regions inside the cone). Solid (dashed) lines are for $a = 1/2$ ($a = 1/3$). For $a = 1/2$, the green shaded region is allowed (similar for $a = 1/3$ using the dashed bounds).

in our case

$$\mathcal{L} \supset \frac{a}{3} \frac{g'^2}{m_{Z'}^2} \bar{q}\gamma^\alpha q \bar{\mu}\gamma_\alpha \mu, \quad \text{with } q \in \{u, d, s, c\}. \quad (68)$$

For positive a , the strongest limit from ATLAS is on the operator $\bar{q}\gamma^\alpha P_L q \bar{\mu}\gamma_\alpha P_R \mu$, providing a 95% C.L. limit of [93]

$$m_{Z'}/g' > 1.4 \text{ TeV} \sqrt{a/(1/3)}, \quad (69)$$

which is weaker than the bounds from C_9 (Eq. (57)).

E. Discussion

The relevant low-energy constraints are collected in Fig. 5. If we want to explain $B \rightarrow K^*\mu^+\mu^-$ and $B \rightarrow K\mu^+\mu^-/B \rightarrow Ke^+e^-$ within 2σ (1σ), we need $a < 1.13$ (0.71) to avoid stringent $B_s-\bar{B}_s$ mixing constraints (taking into account the Z' contribution only). Due to the stronger dependence on a , the B_s -mixing constraints are, however, unproblematic for smaller values of a , and actually in agreement with the whole 2σ range for C_9 for $a \leq 1/3$. Values like $a = 1/2$ or $a = 1/3$ and $m_{Z'}/g' \simeq 2-4$ TeV can therefore easily lead to the required C_9 contribution necessary to explain $B \rightarrow K^*\mu^+\mu^-$ and $R(K)$ (Fig. 5). Note that for these statements we assumed $m_A = m_H$, i.e. only took the Z' contribution to $B_s-\bar{B}_s$ mixing into account. However, for $m_A < m_H$ the bounds get weakened, while they become stronger for $m_A > m_H$ due to the (destructive) constructive interference of the H (A) contribution with the Z' and the SM one.

For $a \leq 1/3$ and $m_{Z'}/g' = \mathcal{O}(\text{TeV})$, direct searches at the LHC cut into the $m_{Z'}$ - g' parameter space that is unconstrained by low-energy processes. We then need $m_{Z'} \gtrsim 2.55$ TeV (2.46 TeV) for $a = 1/2$ ($1/3$) if we want to explain $B \rightarrow K^*\mu^+\mu^-$ and $B \rightarrow K\mu^+\mu^-/B \rightarrow$

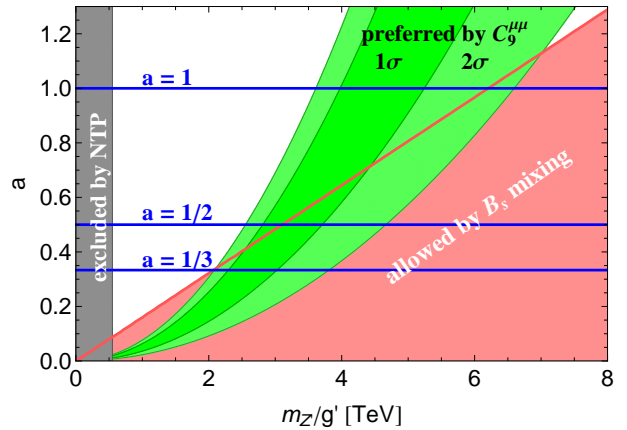


FIG. 5: Limits on $m_{Z'}/g'$ vs. a from NTP (gray), $B_s-\bar{B}_s$ mixing (red), and $C_9^{\mu\mu}$ (green). The horizontal lines indicate some values of interest: $a = 1$, $1/2$, and $1/3$. Not shown are LHC limits (see Fig. 4).

Ke^+e^- within 2σ (Fig. 4)⁴. This also implies a lower limit on the gauge coupling $g' \gtrsim 0.55$ (0.65) for $a = 1/2$ ($1/3$), resulting in a $U(1)'$ Landau pole below 10^{15} GeV (3×10^{12} GeV).

We remark that the dominant flavour violation in the b - s sector also induces the decay $h \rightarrow bs$, with branching ratio of order $10^{-3} \cos^2(\alpha - \beta) \tan^2 \beta$. While generically unobservably small due to the B_s -mixing constraints in Eq. (65), it can be large if the A contribution to Δm_{B_s} takes just the right value.

IV. EXTENSION TO THREE SCALAR DOUBLETS

Above we considered a 2HDM with a horizontal $U(1)'$ gauge symmetry that leads to flavour-violating couplings of h and Z' to quarks and can successfully explain the anomalies in $B \rightarrow K^*\mu^+\mu^-$ and $R(K)$. In this section we will additionally aim at explaining the tantalizing hint for $h \rightarrow \mu\tau$ from CMS [19] (see Eq. (2)), which violates $L_\mu - L_\tau$ by two units. The signal can be accommodated in gauged $U(1)_{L_\mu - L_\tau}$ models by breaking the symmetry with a scalar doublet Ψ_3 carrying $|Q'| = 2$ [32, 33]. Since we cannot set $|a| = 2$ in our 2HDM from above if we want to explain the LHCb anomalies (see Fig. 5), we have to introduce a third doublet that carries $|Q'| = 2$. Thus, in total three scalar doublets,

$$\Psi_j \equiv \begin{pmatrix} \psi_j^+ \\ (v_j + \psi_j^{0,R} - i\psi_j^{0,I})/\sqrt{2} \end{pmatrix}, \quad j = 1, 2, 3, \quad (70)$$

⁴ Note that the ATLAS constraints can also be evaded for $m_{Z'} \ll \text{TeV}$ with much smaller g' (Fig. 4). For $a = 1/2$ ($1/3$), this would require $m_{Z'} < 300$ GeV (400 GeV) and $g' < 0.06$ (0.1), not necessarily compatible with the approximations used above, so we omit a discussion for now.

with $v \equiv \sqrt{v_1^2 + v_2^2 + v_3^2} \simeq 246$ GeV, are introduced to generate viable fermion masses and mixing, as well as the desired lepton-flavor violation in $h \rightarrow \mu\tau$. They have the $U(1)'$ charges

$$Q'(\Psi_1) = -a, \quad Q'(\Psi_2) = 0, \quad Q'(\Psi_3) = -2, \quad (71)$$

respectively. We need again (at least) two singlet scalars to break the $U(1)'$ spontaneously above the electroweak scale. The same arguments from above apply regarding the need for more scalars if $a < 1/3$ is taken.

For simplicity we will again assume a negligible mixing of the doublets Ψ and singlets Φ , as in Sec. II, which makes sense in the limit $\langle \Phi_j \rangle, m_{\Phi_j} \gg \langle \Psi_i \rangle, m_{\Psi_i}$. In this case, we effectively end up with a restricted 3HDM at low energies with a scalar potential

$$\begin{aligned} V \simeq & \sum_{j=1,2,3} \left(m_j^2 |\Psi_j|^2 + \frac{\lambda_j}{2} |\Psi_j|^4 \right) \\ & + \lambda_{12} |\Psi_1|^2 |\Psi_2|^2 + \lambda_{13} |\Psi_1|^2 |\Psi_3|^2 + \lambda_{23} |\Psi_2|^2 |\Psi_3|^2 \\ & + \tilde{\lambda}_{12} |\Psi_1^\dagger \Psi_2|^2 + \tilde{\lambda}_{13} |\Psi_1^\dagger \Psi_3|^2 + \tilde{\lambda}_{23} |\Psi_2^\dagger \Psi_3|^2 \\ & + \left(m_{12}^2 \Psi_1^\dagger \Psi_2 + m_{23}^2 \Psi_2^\dagger \Psi_3 + \text{h.c.} \right). \end{aligned} \quad (72)$$

The mass terms m_{ij}^2 of the last line are of particular importance and are generated by the singlet VEVs $\langle \Phi_j \rangle$; note the absence of a term $m_{13}^2 \Psi_1^\dagger \Psi_3$ and quartic terms like $\Psi_2^\dagger \Psi_1 \Psi_3^\dagger \Psi_3$. Even though it may look complicated, the above potential (with 16 real parameters) is already much simpler than the general 3HDM (with 54 parameters) due to our imposed (and essentially softly broken) $U(1)'$ symmetry.

Compared to the 2HDM from Sec. II, we now need two angles β to parametrize the ratios $\langle \Psi_2 \rangle / \langle \Psi_{1,3} \rangle$, and three angles α to describe the mixing of the three CP-even fields $h, H_{1,2}$. In addition, also the CP-odd fields $A_{1,2}$ and the charged fields $H_{1,2}^+$ mix among each other.

Assuming a CP-conserving potential, i.e. real $m_{12,23}^2$, the minimization conditions give

$$m_2^2 \simeq -\frac{\lambda_2 v_2^2}{2}, \quad m_{12}^2 \simeq -\frac{2m_1^2 v_1}{v_2}, \quad m_{23}^2 \simeq -\frac{2m_3^2 v_3}{v_2}, \quad (73)$$

in the limit $v_2 \gg v_{1,3}$. This limit is particularly useful in this 3HDM because it allows for approximations leading

to rather simple analytic expressions. It is valid because we already know from the above analysis that $v_1 \ll v_2$, and from Refs. [32, 33] that $v_3 \ll v_2$, i.e. we are in the “large $\tan \beta$ ” region in both sectors.

For the pseudo-scalars, the would-be Goldstone boson eaten by the Z is given by $G^0 = \sum_j v_j \psi_j^{0,I} / v$; the pseudo-scalars orthogonal to G^0 further mix due to a complicated 2×2 mass matrix. We write $(A_1, G^0, A_2) = U_A(\psi_1^{0,I}, \psi_2^{0,I}, \psi_3^{0,I})$ with the parametrization

$$\begin{aligned} U_A = & \begin{pmatrix} -1 & & \\ & 1 & \\ & & -1 \end{pmatrix} \begin{pmatrix} 1 & & \\ & \cos \eta_{23} & \sin \eta_{23} \\ & -\sin \eta_{23} & \cos \eta_{23} \end{pmatrix} \\ & \times \begin{pmatrix} \cos \eta_{13} & \sin \eta_{13} \\ & 1 \\ -\sin \eta_{13} & \cos \eta_{13} \end{pmatrix} \begin{pmatrix} \cos \eta_{12} & -\sin \eta_{12} \\ \sin \eta_{12} & \cos \eta_{12} \\ & & 1 \end{pmatrix}. \end{aligned} \quad (74)$$

For $v_{1,3} \ll v_2$, the angles are approximately given by

$$\begin{aligned} \eta_{12} & \simeq \frac{v_1}{v}, \quad \eta_{23} \simeq \frac{v_3}{v}, \\ \eta_{13} & \simeq \frac{v_1 v_3}{v^2} \frac{2m_3^2 + (\lambda_{23} + \tilde{\lambda}_{23})v^2}{2(m_1^2 - m_3^2) + (\lambda_{12} + \tilde{\lambda}_{12} - \lambda_{23} - \tilde{\lambda}_{23})v^2}. \end{aligned} \quad (75)$$

Here, η_{13} is the most complicated angle, but turns out to be small due to $v_1 v_3 \ll v^2$. While it is obvious that the 12 and 23 mixing is small in the limit $v_{1,3} \ll v_2$, it is less obvious why the 13 mixing is so small. The reason is the absence of a term $m_{13}^2 \Psi_1^\dagger \Psi_3$ in the potential, which implies that all 13 mixing originates from the products $v_1 v_3$ of VEVs. We will neglect the mixing in the 13 sector in the following, which drastically simplifies matters. In the limit $v_{1,3} \ll v_2$, we then define the two beta angles $\beta_{12,23} \simeq \pi/2 - \eta_{12,23}$, i.e. $\tan \beta_{ij} \simeq 1/\eta_{ij}$. β_{12} then corresponds to the β angle from above (Sec. II), while β_{23} corresponds to the β angle from Refs. [32, 33] and is hence expected to satisfy $\tan \beta_{23} \gg 1$ (to be quantified below).

The charged fields ψ_j^+ have the same mixing pattern to linear order in $v_{1,3}$: $(H_1^+, G^+, H_2^+) \simeq U_A(\psi_1^+, \psi_2^+, \psi_3^+)$, with would-be Goldstone boson G^+ . Finally, the CP-even fields $(\psi_1^{0,R}, \psi_2^{0,R}, \psi_3^{0,R})$ have a symmetric mass matrix

$$M_S^2 \simeq \begin{pmatrix} m_1^2 + \frac{1}{2}(\lambda_{12} + \tilde{\lambda}_{12})v^2 & \left(\frac{1}{2}(\lambda_{12} + \tilde{\lambda}_{12})v - m_1^2/v \right) v_1 & (\lambda_{13} + \tilde{\lambda}_{13})v_1 v_3 \\ \cdot & \lambda_2 v^2 & \left(\frac{1}{2}(\lambda_{23} + \tilde{\lambda}_{23})v - m_3^2/v \right) v_3 \\ \cdot & \cdot & m_3^2 + \frac{1}{2}(\lambda_{23} + \tilde{\lambda}_{23})v^2 \end{pmatrix}. \quad (77)$$

The mixing is obviously again suppressed by $v_{1,3}/v$; in

particular the 13 mixing is small. We write $(H_1, h, H_2) =$

$U_H(\psi_1^{0,R}, \psi_2^{0,R}, \psi_3^{0,R})$ with

$$U_H \simeq \begin{pmatrix} 1 & & & \\ & \cos \alpha_{23} & -\sin \alpha_{23} & \\ & \sin \alpha_{23} & \cos \alpha_{23} & \\ & & & 1 \end{pmatrix} \begin{pmatrix} \cos \alpha_{12} & \sin \alpha_{12} & & \\ -\sin \alpha_{12} & \cos \alpha_{12} & & \\ & & & \\ & & & 1 \end{pmatrix}, \quad (78)$$

where we already neglected the small 13 mixing. The remaining two scalar mixing angles take the form

$$\alpha_{12} \simeq -\frac{v_1}{v} \frac{2m_1^2 - (\lambda_{12} + \tilde{\lambda}_{12})v^2}{2m_1^2 - 2\lambda_2 v^2 + (\lambda_{12} + \tilde{\lambda}_{12})v^2}, \quad (79)$$

$$\alpha_{23} \simeq -\frac{v_3}{v} \frac{2m_3^2 - (\lambda_{23} + \tilde{\lambda}_{23})v^2}{2m_3^2 - 2\lambda_2 v^2 + (\lambda_{23} + \tilde{\lambda}_{23})v^2}. \quad (80)$$

Keeping in mind that the second and third scalar doublets hardly mix in the limit of interest, our 3HDM simplifies significantly, especially taking into account that Ψ_3 only couples to leptons and Ψ_1 only to quarks. Essentially, our model looks like the 2HDM from Ref. [32] in the lepton sector, *and like a separate 2HDM in the quark sector*. This means we can describe the lepton sector as a type-I-like 2HDM with an angle β_{23} and α_{23} , and the quark sector as a type-I-like 2HDM with angle β_{12} and α_{12} . The scalar doublet Ψ_2 is mostly SM-like and will inherit off-diagonal couplings to $\mu\tau$ from Ψ_3 and to tu , tc , db , sb from Ψ_1 .

In this limit, our 3HDM is parametrized by the masses (m_h , $m_{H_{1,2}}$, $m_{H_{1,2}^+}$, $m_{A_{1,2}}$), the vacuum-angles $\beta_{12,23}$, and the mixing angles $\alpha_{12,23}$ for the CP-even scalars.

A. Quark masses and couplings

For the quark masses and couplings, nothing changes compared to the 2HDM above; we simply replace $\tan \beta \rightarrow \tan \beta_{12} \simeq v/v_1$ and $\alpha \rightarrow \alpha_{12}$, keeping in mind that this only works in the limits of large $\tan \beta_{ij}$ and small α_{ij} . In particular, we can again easily resolve the anomalies in $B \rightarrow K^* \mu^+ \mu^-$ and $B \rightarrow K \mu^+ \mu^- / B \rightarrow K e^+ e^-$ using the flavour violating Z' couplings as discussed above. As we will see below, the additional constraints from the lepton sector (compared to the 2HDM discussed before) do not interfere with this solution. In fact, the additional resolution of $h \rightarrow \mu\tau$ makes possible a prediction for $\tau \rightarrow 3\mu$, depending on C_9 .

B. Lepton masses and couplings

Lepton-flavour violation arises as in Ref. [32], with Ψ_3 playing the role of the non-SM doublet. The Yukawa couplings are given by

$$\mathcal{L} = -\bar{L}_f \left(\xi_{fi}^{\nu R} \tilde{\Psi}_3 + Y_{fi}^{\nu R} \tilde{\Psi}_2 \right) \nu_{R,i} - \bar{L}_f \left(\xi_{fi}^e \Psi_3 + Y_{fi}^e \Psi_2 \right) e_i + \text{h.c.} \quad (81)$$

$Y^{\nu R}$ and Y^e are diagonal due to the $U(1)'$ symmetry, while $\xi^{\nu R, e}$ are given by

$$\xi^{\nu R} = \begin{pmatrix} 0 & 0 & 0 \\ 0 & 0 & \xi_{23} \\ 0 & 0 & 0 \end{pmatrix}, \quad \xi^e = \begin{pmatrix} 0 & 0 & 0 \\ 0 & 0 & 0 \\ 0 & \xi_{\tau\mu} & 0 \end{pmatrix}. \quad (82)$$

The right-handed neutrino mass matrix takes again the form of Eq. (36) with two vanishing entries. However, due to the non-diagonal Dirac matrices, the active neutrino mass matrix no longer features two vanishing minors but only one, softening the fine-tuning to obtain valid mixing parameters. We again expect a quasi-degenerate neutrino mass spectrum and a close-to-maximal atmospheric mixing angle [32] but lose the very specific predictions we obtained in the 2HDM from Sec. IID.

Diagonalization of the charged-lepton mass matrix requires only a small 23 rotation of (μ_R, τ_R) by an angle $\theta_R \simeq \cos \beta_{23} \xi_{\tau\mu} v / \sqrt{2} m_\tau$, while the left-handed angle is suppressed by m_μ / m_τ . The LFV coupling of h is then approximately given by

$$\mathcal{L} \supset -\theta_R \frac{m_\tau}{v} \frac{\cos(\alpha_{23} - \beta_{23})}{\cos \beta_{23} \sin \beta_{23}} \bar{\tau} P_R \mu h + \text{h.c.} \quad (83)$$

A non-zero θ_R hence induces the decay $h \rightarrow \mu\tau$, while any charged LFV involving electrons is forbidden (in the limit of zero neutrino masses). The scalars $-H_2$, A_2 , and H_2^+ – also couple off diagonally to leptons, but their effect in LFV observables is small [32]. The Z' couplings are given by

$$\mathcal{L} \supset g' \left(\bar{e}_i \gamma^\mu P_L e_j Z'_\mu \Gamma_{ij}^{eL} + \bar{e}_i \gamma^\mu P_R e_j Z'_\mu \Gamma_{ij}^{eR} \right), \quad (84)$$

with $\Gamma^{eL} \simeq \text{diag}(0, 1, -1)$ and

$$\Gamma_{fi}^{eR} \simeq \begin{pmatrix} 0 & 0 & 0 \\ 0 & 1 & 2\theta_R \\ 0 & 2\theta_R & -1 \end{pmatrix}. \quad (85)$$

Again, a non-zero θ_R induces LFV in the μ - τ sector, mediated by the Z' .

C. Lepton-flavour violation

Concerning LFV we can directly rely on the analysis of Refs. [32, 33]. The branching ratio for $h \rightarrow \mu\tau$ reads

$$\text{Br}[h \rightarrow \mu\tau] \simeq \frac{m_h}{8\pi\Gamma_{\text{SM}}} |\Gamma_{\tau\mu}^h|^2 \simeq 1\% \left(\frac{\theta_R}{0.1} \right)^2 \left(\frac{\cos(\alpha_{23} - \beta_{23})}{0.2} \right)^2 \left(\frac{\tan \beta_{23}}{20} \right)^2, \quad (86)$$

where $\Gamma_{\text{SM}} \simeq 4.1 \text{ MeV}$ is the decay width in the SM for a 125 GeV Brout–Englert–Higgs boson and $\Gamma_{\tau\mu}^h$ is given by the $\bar{\tau} P_R \mu h$ prefactor in Eq. (83).

LFV mediated by Z' most importantly induces the decay $\tau \rightarrow 3\mu$, with $\tau \rightarrow \mu\gamma$ suppressed by an additional factor $2\alpha_{\text{EM}}/\pi$ [33]. The branching ratio is given by

$$\text{Br}[\tau \rightarrow 3\mu] \simeq \frac{m_\tau^5 \theta_R^2}{128\pi^3 \Gamma_\tau} \frac{g'^4}{m_{Z'}^4} \simeq 10^{-8} \left(\frac{\theta_R}{0.1} \right)^2 \left(\frac{6.6 \text{ TeV}}{m_{Z'}/g'} \right)^4, \quad (87)$$

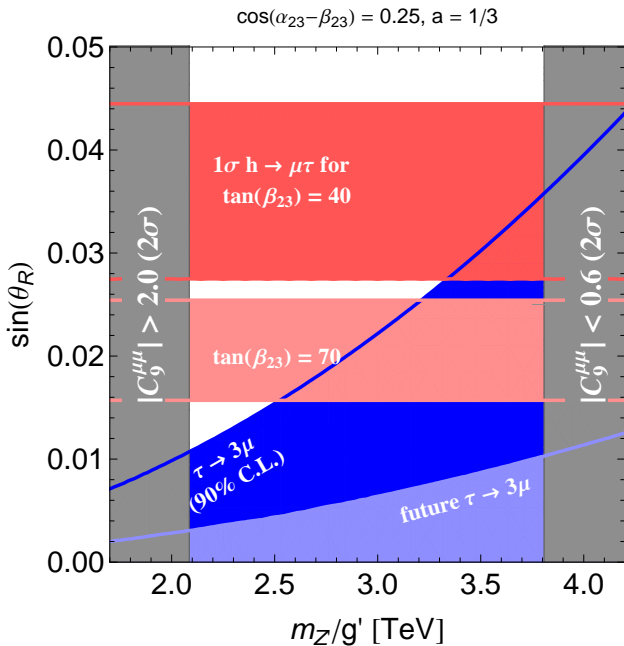


FIG. 6: Allowed regions in the $m_{Z'}/g' - \sin(\theta_R)$ plane for $a = 1/3$: the horizontal stripes correspond to $h \rightarrow \mu\tau$ (1σ) for $\tan\beta_{23} = 70, 40$ and $\cos(\alpha_{23} - \beta_{23}) = 0.25$, and (light) blue stands for (future) $\tau \rightarrow 3\mu$ limits at 90% C.L. The gray regions are excluded by the 2σ range for $C_9^{\mu\mu}$ (see Eq. (56)). In this range, ATLAS limits constrain $m_{Z'} \gtrsim 2.5$ TeV (see Fig. 4).

which has to be compared to the current upper limit of 1.2×10^{-8} at 90% C.L. which is obtained from combining data from Belle and BaBar [94]. This limit can most likely be improved by an order of magnitude to 10^{-9} in the future [95].

In the previous sections, we have seen that a resolution of the B -meson anomalies – indicated through a non-zero C_9 (Eq. (56)) – requires $m_{Z'}/g'$ to be in the TeV range (Fig. 5). In Fig. 6 we show the exclusion limits from $\tau \rightarrow 3\mu$ together with the preferred region for $h \rightarrow \mu\tau$ and the C_9 constraints on $m_{Z'}/g'$. The important part is the upper limit on $m_{Z'}/g'$ from C_9 . With a non-zero value for θ_R required by $h \rightarrow \mu\tau$, we can then predict a rate for $\tau \rightarrow 3\mu$ mediated by the Z' . For this we express $m_{Z'}/g'$ in terms of C_9 and θ_R in $\text{Br}[h \rightarrow \mu\tau]$ to arrive at

$$\text{Br}[\tau \rightarrow 3\mu] \simeq 4.6 \times 10^{-5} \frac{C_9^2 \cos^2 \beta_{23} \sin^2 \beta_{23}}{a^2 \cos^2(\alpha_{23} - \beta_{23})} \text{Br}[h \rightarrow \mu\tau]. \quad (88)$$

We remind the reader that the angles α_{23} and β_{23} do not correspond to the 2HDM angles from Sec. II but to those from Refs. [32, 33]. Using the 2σ lower limits on C_9 (Eq. (56)) and $h \rightarrow \mu\tau$ (Eq. (2)), as well as the LHC constraint $|\cos(\alpha_{23} - \beta_{23})| \leq 0.4$ [74, 75], we can predict

$$\text{Br}[\tau \rightarrow 3\mu] \gtrsim 9.3 \times 10^{-9} \left(\frac{10}{\tan \beta_{23}} \right)^2, \quad (89)$$

working in the large $\tan \beta_{23}$ limit and setting $a = 1/3$. The current bound is then $\tan \beta_{23} \gtrsim 9$, while the future

reach goes above $\tan \beta_{23} \sim 30$. Using the 1σ limits for C_9 and $h \rightarrow \mu\tau$ gives a current (future) bound of 30 (104) on $\tan \beta_{23}$. This is much stronger than the prediction of Ref. [33] in a model with vector-like quarks, where 1σ limits only implied a future reach up to $\tan \beta \sim 60$ (using the updated value for $h \rightarrow \mu\tau$ from Eq. (2)). The 3HDM with gauged horizontal $U(1)'$ charges studied here is hence more tightly constrained than the 2HDM with vector-like quarks [33].

Equation (89) is the main prediction of the simultaneous explanation of the B -meson anomalies in connection with $h \rightarrow \mu\tau$. Note that in addition to the $m_{Z'}/g'$ limits from C_9 , ATLAS constrains $m_{Z'}$ vs. g' (Fig. 4). For the parameters in Fig. 6, this imposes the additional bound $m_{Z'} \gtrsim 2.5$ TeV (or $g' \gtrsim 0.65$), which puts the $U(1)'$ Landau pole below roughly 3×10^{12} GeV for $a = 1/3$.

V. CONCLUSIONS AND OUTLOOK

In this paper we proposed a model with multiple scalar doublets and a horizontal $U(1)'$ gauge symmetry in which all three LHC anomalies in the flavour sector ($B \rightarrow K^* \mu^+ \mu^-$, $R(K)$ and $h \rightarrow \mu\tau$) can be explained simultaneously. Compared to previous explanations, our model does not require vector-like quarks charged under the new gauge group. The spontaneously broken anomaly-free $U(1)'$ gauge symmetry is generated by

$$Q' = (L_\mu - L_\tau) - a(B_1 + B_2 - 2B_3), \quad a \in \mathbb{Q}, \quad (90)$$

which leads to successful fermion-mixing patterns. In particular, it generates a large (small) atmospheric (reactor) mixing angle in the lepton sector and explains the almost decoupled third quark generation. The universal charges the quarks of the first two generations allow for the generation of the Cabibbo angle without dangerously large effects in Kaon mixing, and the neutrality of electrons under the $U(1)'$ symmetry softens constraints without fine-tuning.

The observed quark mixing of the CKM matrix requires the $U(1)'$ to be broken with a second scalar doublet with $U(1)'$ charge $-a$, which leads to flavour-violating couplings of the Z' and of the scalars, giving simultaneously a natural explanation for the smallness of V_{ub} and V_{cb} . Scalar contributions to $B_s - \bar{B}_s$ mixing typically require $\alpha - \beta \simeq \pi/2$, which is, however, relaxed for $m_A < m_H$. The anomalies in $B \rightarrow K^* \mu^+ \mu^-$ and $R(K)$ can be explained with a TeV-scale Z' boson and $a < 1$ while satisfying $B_s - \bar{B}_s$ -mixing constraints and limits from direct Z' searches at the LHC. Future LHC and FCC (Future Circular Collider) searches are very interesting for our model as they might strengthen the current limits or lead to the discovery of the Z' boson.

Introducing a third scalar doublet, with $U(1)'$ charge -2 , gives rise to the decay $h \rightarrow \mu\tau$ in complete analogy to Refs. [32, 33]. Together with the large Z' effect necessary to resolve $B \rightarrow K^* \mu^+ \mu^-$ and $R(K)$, the decay $h \rightarrow \mu\tau$ then allows us to predict a rate for $\tau \rightarrow 3\mu$, depending on $\tan \beta$ and $\cos(\alpha - \beta)$, potentially measurable in future experiments.

Acknowledgments

We thank Gennaro Corcella for useful discussions concerning LHC bounds on Z' models and Ulrich Haisch for useful comments on the manuscript. A. Crivellin is supported by a Marie Curie Intra-European Fellowship of the European Community's 7th Framework Programme under contract number PIEF-GA-2012-326948. G. D'Ambrosio acknowledges the partial support my MIUR under the project number 2010YJ2NYW. The work of J. Heeck is funded in part by IISN and by Belgian Science Policy (IAP VII/37).

Note added: During the publication process of this article, new LHCb results were presented at the *Rencontres de Moriond Electroweak Session 2015* which hint at a confirmation of the anomaly in $B \rightarrow K^* \mu^+ \mu^-$. The global fit now prefers new physics in $C_9^{\mu\mu}$ over the Standard Model by 4.3σ [96].

Appendix A: Other horizontal symmetries

Demanding a universal $U(1)'$ quark coupling to the first two generations and a good flavor symmetry in the lepton sector does not uniquely single out our model with $B_1 + B_2 - 2B_3$ and $L_\mu - L_\tau$. It is well known that, be-

sides $L_\mu - L_\tau$ (which is connected to quasi-degenerate neutrinos), the symmetries L_e and $L_e - L_\mu - L_\tau$ are good zeroth-order approximations for a neutrino mass matrix with normal and inverted hierarchy, respectively [55]. Since these two are anomalous, one can consider $B - 3L_e$ [97, 98] or $B + 3(L_e - L_\mu - L_\tau)$ [99, 100] as well-motivated gauge symmetries. With non-universal quark charges – but universal in the first two generations – we can consider $B_3 - L_e$ or $B_3 + (L_e - L_\mu - L_\tau)$ as anomaly-free gauge symmetries that provide a successful neutrino mixing, single out the third quark generation, and lead to LFV in both lepton and quark sectors. Quite analogously one can consider the lepton symmetries from Ref. [59] with a non-universal quark charge, which lead to predictive texture zeros and vanishing minors in the neutrino mass matrix; for example, $3B_3 + L_e - 3L_\mu - L_\tau$ generates the texture zeros $(m_\nu)_{11} = 0 = (m_\nu)_{13}$ after seesaw. While all these symmetries are interesting in their own right, they are not useful for our purpose because the Z' coupling to quarks compared to muons is rather large (and not adjustable), so it becomes difficult to generate a large C_9 without violating B - \bar{B} -mixing bounds. In addition, any Z' that couples to electrons unavoidably suffers from stringent LEP constraints [87]. The horizontal gauge symmetry $(L_\mu - L_\tau) - a(B_1 + B_2 - 2B_3)$ chosen in this paper is hence a remarkably good choice to address the existing hints for flavour violation.

-
- [1] G. Aad et al. (ATLAS Collaboration), Phys.Lett. **B716**, 1 (2012), 1207.7214.
 - [2] S. Chatrchyan et al. (CMS Collaboration), Phys.Lett. **B716**, 30 (2012), 1207.7235.
 - [3] R. Aaij et al. (LHCb collaboration), Phys.Rev.Lett. **111**, 191801 (2013), 1308.1707.
 - [4] S. Descotes-Genon, T. Hurth, J. Matias, and J. Virto, JHEP **1305**, 137 (2013), 1303.5794.
 - [5] S. Descotes-Genon, L. Hofer, J. Matias, and J. Virto, JHEP **1412**, 125 (2014), 1407.8526.
 - [6] W. Altmannshofer and D. M. Straub (2014), 1411.3161.
 - [7] S. Jäger and J. Martin Camalich (2014), 1412.3183.
 - [8] S. Descotes-Genon, J. Matias, and J. Virto, Phys.Rev. **D88**, 074002 (2013), 1307.5683.
 - [9] W. Altmannshofer and D. M. Straub, Eur.Phys.J. **C73**, 2646 (2013), 1308.1501.
 - [10] R. R. Horgan, Z. Liu, S. Meinel, and M. Wingate, Phys.Rev.Lett. **112**, 212003 (2014), 1310.3887.
 - [11] J. Lyon and R. Zwicky (2014), 1406.0566.
 - [12] R. Aaij et al. (LHCb collaboration), Phys.Rev.Lett. **113**, 151601 (2014), 1406.6482.
 - [13] C. Bobeth, G. Hiller, and G. Piranishvili, JHEP **0712**, 040 (2007), 0709.4174.
 - [14] T. Hurth, F. Mahmoudi, and S. Neshatpour, JHEP **1412**, 053 (2014), 1410.4545.
 - [15] R. Alonso, B. Grinstein, and J. Martin Camalich, Phys.Rev.Lett. **113**, 241802 (2014), 1407.7044.
 - [16] G. Hiller and M. Schmaltz, Phys.Rev. **D90**, 054014 (2014), 1408.1627.
 - [17] D. Ghosh, M. Nardecchia, and S. Renner, JHEP **1412**, 131 (2014), 1408.4097.
 - [18] B. Bhattacharya, A. Datta, D. London, and S. Shivashankara, Phys.Lett. **B742**, 370 (2015), 1412.7164.
 - [19] V. Khachatryan et al. (CMS Collaboration) (2015), 1502.07400.
 - [20] CMS (CMS Collaboration) (2014), CMS-PAS-HIG-14-005.
 - [21] R. Harnik, J. Kopp, and J. Zupan, JHEP **1303**, 026 (2013), 1209.1397.
 - [22] G. Blankenburg, J. Ellis, and G. Isidori, Phys.Lett. **B712**, 386 (2012), 1202.5704.
 - [23] S. Davidson and P. Verrier, Phys.Rev. **D86**, 111701 (2012), 1211.1248.
 - [24] A. Arhrib, Y. Cheng, and O. C. Kong, Phys.Rev. **D87**, 015025 (2013), 1210.8241.
 - [25] A. Arhrib, Y. Cheng, and O. C. Kong, Europhys.Lett. **101**, 31003 (2013), 1208.4669.
 - [26] A. Falkowski, D. M. Straub, and A. Vicente, JHEP **1405**, 092 (2014), 1312.5329.
 - [27] A. Celis, V. Cirigliano, and E. Passemar (2014), 1409.4439.
 - [28] J. Kopp and M. Nardecchia, JHEP **1410**, 156 (2014), 1406.5303.
 - [29] L. de Lima, C. S. Machado, R. D. Matheus, and L. A. F. d. Prado (2015), 1501.06923.
 - [30] M. D. Campos, A. E. C. Hernández, H. Päs, and E. Schumacher (2014), 1408.1652.
 - [31] D. Aristizabal Sierra and A. Vicente, Phys.Rev. **D90**, 115004 (2014), 1409.7690.
 - [32] J. Heeck, M. Holthausen, W. Rodejohann, and Y. Shimizu (2014), 1412.3671.
 - [33] A. Crivellin, G. D'Ambrosio, and J. Heeck, Phys.Rev.Lett. **114**, 151801 (2015), 1501.00993.
 - [34] I. Dorsner, S. Fajfer, A. Greljo, J. F. Kamenik, N. Kos-

- nik, et al. (2015), 1502.07784.
- [35] Y. Omura, E. Senaha, and K. Tobe (2015), 1502.07824.
- [36] A. Dery, A. Efrati, Y. Nir, Y. Soreq, and V. Susi, *Phys.Rev.* **D90**, 115022 (2014), 1408.1371.
- [37] C.-J. Lee and J. Tandean (2014), 1410.6803.
- [38] B. Gripaos, M. Nardecchia, and S. Renner (2014), 1412.1791.
- [39] S. Sahoo and R. Mohanta (2015), 1501.05193.
- [40] R. Gauld, F. Goertz, and U. Haisch, *Phys.Rev.* **D89**, 015005 (2014), 1308.1959.
- [41] A. J. Buras and J. Girrbach, *JHEP* **1312**, 009 (2013), 1309.2466.
- [42] R. Gauld, F. Goertz, and U. Haisch, *JHEP* **1401**, 069 (2014), 1310.1082.
- [43] A. J. Buras, F. De Fazio, and J. Girrbach, *JHEP* **1402**, 112 (2014), 1311.6729.
- [44] W. Altmannshofer, S. Gori, M. Pospelov, and I. Yavin, *Phys.Rev.* **D89**, 095033 (2014), 1403.1269.
- [45] P. Langacker and M. Plumacher, *Phys.Rev.* **D62**, 013006 (2000), hep-ph/0001204.
- [46] V. Barger, C.-W. Chiang, P. Langacker, and H.-S. Lee, *Phys.Lett.* **B580**, 186 (2004), hep-ph/0310073.
- [47] K. Cheung, C.-W. Chiang, N. Deshpande, and J. Jiang, *Phys.Lett.* **B652**, 285 (2007), hep-ph/0604223.
- [48] V. Barger, L. Everett, J. Jiang, P. Langacker, T. Liu, et al., *Phys.Rev.* **D80**, 055008 (2009), 0902.4507.
- [49] V. Barger, L. L. Everett, J. Jiang, P. Langacker, T. Liu, et al., *JHEP* **0912**, 048 (2009), 0906.3745.
- [50] X. He, G. C. Joshi, H. Lew, and R. Volkas, *Phys.Rev.* **D43**, 22 (1991).
- [51] R. Foot, *Mod.Phys.Lett.* **A6**, 527 (1991).
- [52] X.-G. He, G. C. Joshi, H. Lew, and R. Volkas, *Phys.Rev.* **D44**, 2118 (1991).
- [53] P. Binetruy, S. Lavignac, S. T. Petcov, and P. Ramond, *Nucl.Phys.* **B496**, 3 (1997), hep-ph/9610481.
- [54] N. F. Bell and R. R. Volkas, *Phys.Rev.* **D63**, 013006 (2000), hep-ph/0008177.
- [55] S. Choubey and W. Rodejohann, *Eur.Phys.J.* **C40**, 259 (2005), hep-ph/0411190.
- [56] J. Heck and W. Rodejohann, *Phys.Rev.* **D84**, 075007 (2011), 1107.5238.
- [57] G. Dutta, A. S. Joshipura, and K. Vijaykumar, *Phys.Rev.* **D50**, 2109 (1994), hep-ph/9405292.
- [58] J.-Y. Liu, Y. Tang, and Y.-L. Wu, *J.Phys.* **G39**, 055003 (2012), 1108.5012.
- [59] T. Araki, J. Heck, and J. Kubo, *JHEP* **1207**, 083 (2012), 1203.4951.
- [60] J. Heck and W. Rodejohann, *Phys.Lett.* **B705**, 369 (2011), 1109.1508.
- [61] G. Branco, P. Ferreira, L. Lavoura, M. Rebelo, M. Sher, et al., *Phys.Rept.* **516**, 1 (2012), 1106.0034.
- [62] S. Descotes-Genon, J. Matias, and J. Virto, *PoS EPS-HEP2013*, 361 (2013), 1311.3876.
- [63] C.-W. Chiang, N. Deshpande, and J. Jiang, *JHEP* **0608**, 075 (2006), hep-ph/0606122.
- [64] M. Gonzalez-Garcia, M. Maltoni, and T. Schwetz, *JHEP* **1411**, 052 (2014), updated version 2.0 from <http://www.nu-fit.org>, 1409.5439.
- [65] M. Agostini et al. (GERDA Collaboration), *Phys.Rev.Lett.* **111**, 122503 (2013), 1307.4720.
- [66] P. Ade et al. (Planck Collaboration), *Astron.Astrophys.* **571**, A16 (2014), 1303.5076.
- [67] P. Ade et al. (Planck Collaboration) (2015), 1502.01589.
- [68] P. Minkowski, *Phys.Lett.* **B67**, 421 (1977).
- [69] L. Lavoura, *Phys.Lett.* **B609**, 317 (2005), hep-ph/0411232.
- [70] E. Lashin and N. Chamoun, *Phys.Rev.* **D78**, 073002 (2008), 0708.2423.
- [71] K. Abazajian et al., *Astropart.Phys.* **63**, 66 (2015), 1309.5383.
- [72] S. Bilenky and C. Giunti, *Int.J.Mod.Phys.* **A30**, 1530001 (2015), 1411.4791.
- [73] P. Langacker, *Rev.Mod.Phys.* **81**, 1199 (2009), 0801.1345.
- [74] B. Dumont, J. F. Gunion, Y. Jiang, and S. Kraml, *Phys.Rev.* **D90**, 035021 (2014), 1405.3584.
- [75] B. Dumont, J. F. Gunion, Y. Jiang, and S. Kraml (2014), 1409.4088.
- [76] M. Ciuchini, E. Franco, V. Lubicz, G. Martinelli, I. Scimemi, et al., *Nucl.Phys.* **B523**, 501 (1998), hep-ph/9711402.
- [77] A. Crivellin, A. Kokulu, and C. Greub, *Phys.Rev.* **D87**, 094031 (2013), 1303.5877.
- [78] S. Aoki, Y. Aoki, C. Bernard, T. Blum, G. Colangelo, et al., *Eur.Phys.J.* **C74**, 2890 (2014), 1310.8555.
- [79] A. J. Buras, M. Misiak, and J. Urban, *Nucl.Phys.* **B586**, 397 (2000), hep-ph/0005183.
- [80] M. Bona et al. (UTfit Collaboration), UTfit homepage <http://utfit.org> (2014).
- [81] M. Bona et al. (UTfit Collaboration), *Phys.Rev.Lett.* **97**, 151803 (2006), hep-ph/0605213.
- [82] M. Bona et al. (UTfit Collaboration), *JHEP* **0803**, 049 (2008), 0707.0636.
- [83] J. Charles et al. (CKMfitter Group), *Eur.Phys.J.* **C41**, 1 (2005), hep-ph/0406184.
- [84] C.-Y. Chen and S. Dawson, *Phys.Rev.* **D87**, 055016 (2013), 1301.0309.
- [85] W. Altmannshofer, S. Gori, M. Pospelov, and I. Yavin, *Phys.Rev.Lett.* **113**, 091801 (2014), 1406.2332.
- [86] S. Mishra et al. (CCFR Collaboration), *Phys.Rev.Lett.* **66**, 3117 (1991).
- [87] J. Heck, *Phys.Lett.* **B739**, 256 (2014), 1408.6845.
- [88] G. Aad et al. (ATLAS Collaboration), *Phys.Rev.* **D90**, 052005 (2014), auxiliary figures from <http://atlas.web.cern.ch/Atlas/GROUPS/PHYSICS/PAPERS/EXOT-2012-23/>, 1405.4123.
- [89] E. Ma, D. Roy, and S. Roy, *Phys.Lett.* **B525**, 101 (2002), hep-ph/0110146.
- [90] K. Harigaya, T. Igari, M. M. Nojiri, M. Takeuchi, and K. Tobe, *JHEP* **1403**, 105 (2014), 1311.0870.
- [91] F. del Aguila, M. Chala, J. Santiago, and Y. Yamamoto, *JHEP* **1503**, 059 (2015), 1411.7394.
- [92] N. F. Bell, Y. Cai, R. K. Leane, and A. D. Medina, *Phys.Rev.* **D90**, 035027 (2014), 1407.3001.
- [93] G. Aad et al. (ATLAS Collaboration), *Eur.Phys.J.* **C74**, 3134 (2014), 1407.2410.
- [94] Y. Amhis et al. (Heavy Flavor Averaging Group (HFAG)) (2014), 1412.7515.
- [95] T. Aushev, W. Bartel, A. Bondar, J. Brodzicka, T. Browder, et al. (2010), 1002.5012.
- [96] W. Altmannshofer and D. M. Straub (2015), 1503.06199.
- [97] E. Ma, D. Roy, and U. Sarkar, *Phys.Lett.* **B444**, 391 (1998), hep-ph/9810309.
- [98] E. Salvioni, A. Strumia, G. Villadoro, and F. Zwirner, *JHEP* **1003**, 010 (2010), 0911.1450.
- [99] H.-S. Lee and E. Ma, *Phys.Lett.* **B688**, 319 (2010), 1001.0768.
- [100] J. Heck and W. Rodejohann, *Phys.Rev.* **D85**, 113017 (2012), 1203.3117.